Communication

A Model-Free Output Feedback Control Approach for the Stabilization of Underactuated TORA System with Input Saturation

Changzhong Pan *, Chenchen Cui, Lan Zhou, Peiyin Xiong and Zhijing Li

School of Information and Electrical Engineering, Hunan University of Science and Technology, Xiangtan 411201, China; 15286989175@163.com (C.C.); zhoulan75@163.com (L.Z.); xiongpeiyin@126.com (P.X.); lizhijingwei@163.com (Z.L.)
* Correspondence: pancz@hnust.edu.cn

Abstract: The horizontal translational oscillator with a rotational actuator (TORA) is a typical underactuated mechanical system, whose control problem is still open and theoretically challenging. At present, the existing control methods are structurally complicated and require an exact knowledge of the system parameters. Moreover, few works have considered the output feedback stabilization of the TORA system subject to practical constraints of input saturation and angular velocity unmeasurement. To address these problems, this paper proposes a novel model-free amplitude-limited control approach to stabilize the TORA system at the origin using only angle feedback. Firstly, the passivity of the horizontal TORA system is analyzed, based on which a novel Lyapunov function augmented with an auxiliary signal is constructed by taking the input saturation into account. Then, an amplitude-limited control law is derived in a straightforward manner. In order to make the control law independent of velocity feedback, the auxiliary signal is designed in terms of the ball rotational angle and an output of a dynamic system. The asymptotic stability of the entire control system is rigorously guaranteed by utilizing Lyapunov theory and LaSalle's invariance principle. Finally, simulation results with comparisons to existing methods demonstrate the effectiveness and superiority of the proposed control approach.

Keywords: TORA; underactuated system; output feedback control; input saturation; passivity-based control

1. Introduction

The translational oscillator with a rotational actuator (TORA) was originally developed for studying the resonance capture phenomenon and the despin maneuver for dual-spin spacecrafts [1–3]. It thus has great research significance in aerospace. Currently, the TORA system is used as an active mass damper (AMD) for the active vibration suppression of large practical engineering systems such as super-high-rise buildings, long-span bridges, and offshore floating wind turbines [4–6]. In addition, after extension, it can also be used to the study the self-synchronized phenomenon of many mechanical systems [7], e.g., vibration sifters, handheld vibration tools, vibration conveyors, etc. As shown in Figure 1, the TORA system is composed of an unactuated translational cart and an actuated rotational eccentric ball. Under the drive of a motor, the eccentric ball can rotate around a pivot fixed on the cart while the translational cart oscillates horizontally. Since there are two degrees of freedom (DOFs) needing to be controlled with only one control input, the TORA system becomes a typical underactuated mechanical system (UMS), the merits of which include light weight, simple structure, low manufacturing costs, low energy consumption, and so on [8–14]. Therefore, the study of the TORA system is practically interesting and meaningful.

However, the inherent underactuation feature also brings strong nonlinear state coupling relationship between the translational position and rotational angle, which makes the

control design much more difficult. Since traditional control strategies are not effective for this system any more, various advanced nonlinear control techniques should be explored and developed. From the viewpoint of theoretical control, the TORA system is considered as an ideal benchmark for verifying the effectiveness and feasibility of advanced control algorithms [15–19]. At present, the control problem of underactuated systems including the TORA system is still open and theoretically challenging, which deserves further research.
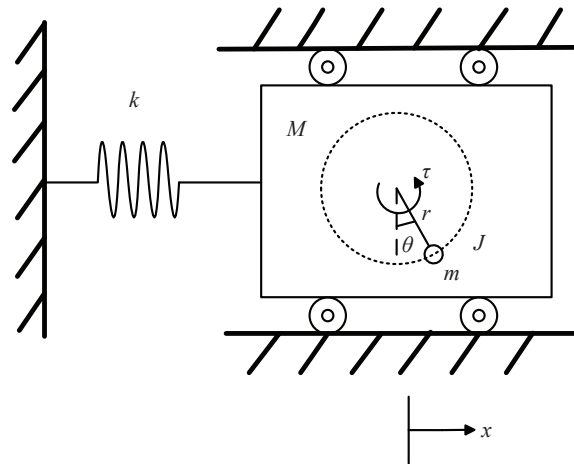

Figure 1. Structure diagram of underactuated horizontal TORA system.

During the past few decades, significant efforts have been made to the research of under-actuated systems, and many effective control approaches have been proposed [10–14,20–22]. Specifically, for the the stabilization control of the TORA system, which is to stabilize both the cart position and the eccentric ball angle at the equilibrium point, the proposed control approaches could be roughly classified into two categories: cascade-based methods and passivity-based methods. The cascade-based methods mainly rely on a cascade model of the TORA system obtained by a series of coordinate transformations, and then advanced control techniques, such as backstepping [23,24], dynamic surface control [25], sliding mode control [17,26,27], positive-definite Lyapunov funtion [28], etc., are incorporated into the controller design. However, the control algorithms developed in these results are stucturely complicated since they require complex coordinate transformations. In addition, the performances of the controllers are sensitive to system parameters, which means the robustness of the control system would be degraded if the knowledge of system parameters is not obtained exactly.

The passivity-based methods are in light of the passive property of the TORA system, which does not need any state transformations. In [29], the total energy of the TORA is employed to show the passivity property, based on which a proper Lyapunov function including energy item is designed, and a state-feedback controller is proposed. In [30], an adaptive controller along with an online estimation mechanism is proposed by using a passivity-based Lyapunov storage function. The control algorithms developed in these results are quite simple, but they require full state feedback, that is, all the system states are assumed to be measurable. In practical applications, however, the velocity feedback is always unavailable due to space, weight, cost constraints and other factors. In order to avoid using velocity feedback, a high-pass filtering approach is proposed for the TORA system in [31]. By employing the techniques of energy shaping and damping injection, an output feedback global stabilization control approach is presented in [32] on the basis of the passivity of the TORA system. For a two-dimensional (2D) TORA system, a number of different types of output feedback controllers are proposed in [33–36] in view of the passive property by assuming that the angular velocity is unavailable.

Besides the abovementioned control methods, some other strategies, including fuzzy control [37,38], hybrid control [39], equivalent input disturbance (EID) control [40], observer-based control [41], have also been proposed for the stabilization of the TORA system.

Although the existing control methods have considered the output feedback (i.e., with no velocity signals) problem, few results take the input saturation into account. In practical applications, input saturation is ubiquitous since control torques provided by actuators are restricted physically [42]. When the input saturation is ignored, it may cause control performance degradation, lag, over-shoot, undershoot as well as instability [43] in the closed-loop control system.

Motivated by the above analysis and observations, this paper aims to directly tackle the output feedback stabilization control problem of the underactuated TORA system subject to input saturation. To this end, a novel model-free energy-based control method is proposed. Specifically, the dynamic model of the TORA system is first given, and the passivity property is analyzed. Then, taking the input saturation into account, an energy-based Lyapunov function augmented with an auxiliary signal is constructed, and an amplitude-limited control law is derived. In order to make the control law independent of velocity feedback, the auxiliary signal is designed in terms of the ball rotational angle and an output of a dynamic system. The stability of the resulting closed-loop control system is guaranteed by the use of Lyapunov theory and LaSalle's invariance principle, which proves rigorously that the TORA system is globally asymptotically stable at the equilibrium point. Finally, numerical simulations with comparisons to existing control methods are carried out to show the control performance of the proposed controller. The results show that a satisfactory and superior control performance is obtained.

Different from the existing control methods, the main merits of this paper lies in the following three aspects:

(1) The proposed control method does not need any coordinate transformations, which results in a very simple structure of the controller. This makes the control algorithm convenient for engineering implementations.

(2) The TORA system is stabilized globally at the the equilibrium point using only output feedback while simultaneously physical control input saturation is taken into account. In other words, no velocity feedback is involved in the proposed controller, and the required control torque never exceeds the amplitude-limited constraint that the actuator can provide.

(3) The proposed controller is model-free, i.e., no system parameters are involved, which makes it insensitive to parameter uncertainties. This improves the robustness of the controller to some extent.

The rest of this paper is organized as follows. In Section 2, the dynamic model of the TORA system is first given, and then the corresponding control problem is formulated. The controller design and the stability analysis of the closed-loop control system are detailed in Section 3. In Section 4, simulation comparisons demonstrate the effectiveness and superiority of the proposed control method. Section 5 summarizes the main work of this paper.

2. Dynamics and Control Problem of the TORA System

The TORA was first proposed in [1,44] as a benchmark system for nonlinear control design. In this paper, we focus on addressing the stabilization issue of the TORA system operated in the horizontal plane with only output (i.e., no velocity) feedback in the presence of amplitude-limited control torque.

As shown in Figure 1, the horizontal TORA system consists of an unactuated cart and an actuated eccentric ball. The cart, which is connected to a fixed wall through a linear spring, moves in a translational orbit, and the ball directly controlled by the actuator rotates in a circle orbit. Using Euler–Lagrange modeling method, the dynamic equations of the horizontal TORA system are obtained as follows [16,32,44]:

$$(M + m)\ddot{x} + mr\ddot{\theta}\cos\theta - mr\dot{\theta}^2\sin\theta + kx = 0, \tag{1}$$

$$mr\ddot{x}\cos\theta + (mr^2 + J)\ddot{\theta} = \tau. \tag{2}$$

where M and m are the masses of the translational cart and the rotational eccentric ball, respectively, x represents the displacement of the cart from the position of the equilibrium point, r is the rotational radius, which takes the counterclockwise rotation direction as the positive direction, θ is the rotation angle of the eccentric ball with respect to the vertical position, J is the moment of inertia of the rotational ball, k denotes the stiffness coefficient of the spring, τ is the control torque of the system. Notice that the TORA system has one control input τ and two configuration variables (x, θ), which makes the system a benchmark example of underactuated mechanical systems.

The total mechanical energy of the horizontal TORA system is expressed as

$$E = \frac{1}{2}(M + m)\dot{x}^2 + mr\dot{x}\dot{\theta}\cos\theta + \frac{1}{2}(mr^2 + J)\dot{\theta}^2 + \frac{1}{2}kx^2 \geq 0. \tag{3}$$

Taking the time derivative of (3) along Equations (1) and (2) yields

$$\dot{E} = \dot{\theta}\tau, \tag{4}$$

which indicates that the TORA system is passive dissipative, and passivity-based controllers can be designed according to this property. However, for practical applications, there are two issues that must be considered. On the one hand, the velocity feedback is always unavailable due to space, weight and cost constraints, plus other factors. On the other hand, the actuator applied to the ball can only provide limited control torque, which means

$$|\tau(t)| \leq \tau_{\max}, \tag{5}$$

where $\tau_{\max} > 0$ represents the maximum torque.

Therefore, the control problem of this paper is formulated as following. *Consider the underactuated horizontal TORA system described by (1) and (2) with the control input restricted by (5). Design a suitable output feedback controller such that all state variables of the TORA system are stabilized at the origin (equilibrium point), which is given by*

$$\lim_{t \to \infty}[x,\ \dot{x},\ \theta,\ \dot{\theta}]^{\mathrm{T}} = [0,\ 0,\ 2n\pi,\ 0]^{\mathrm{T}}. \tag{6}$$

In other words, the translational oscillations of the cart are eliminated while the rotation angle of the ball returns to zero.

3. Model-Free Output Feedback Controller Design

To achieve the aforementioned control objective, this section presents a novel design method of an output feedback controller in the presence of input saturation, and then provides rigorous theoretical stability analysis of the corresponding closed-loop system by Lyapunov theory and LaSalle's invariance principle.

Firstly, based on the passive dissipation characteristics of (4), the following novel energy-based Lyapunov function is constructed

$$V = E + 4k_1 \sin^2(0.25\theta) + \log[\cosh(\phi)], \tag{7}$$

where $k_1 > 0$ is a control design parameter, ϕ is an auxiliary signal which is introduced to avoid the velocity feedback issue, and it will be designed latter. Taking the time derivative of (7) and using (4) yields

$$\begin{aligned}\dot{V} &= \dot{\theta}\tau + 2k_1\dot{\theta}\sin(0.25\theta)\cos(0.25\theta) + \tanh(\phi)\dot{\phi} \\ &= \dot{\theta}\cdot[\tau + k_1\sin(0.5\theta)] + \tanh(\phi)\dot{\phi}.\end{aligned} \tag{8}$$

By choosing a suitable output feedback control law for τ as

$$\tau = -k_1\sin(0.5\theta) - k_2\tanh(\phi), \tag{9}$$

where $k_2 > 0$ is the control gain, we obtain

$$\dot{V} = -k_2 \tanh(\phi)\dot{\theta} + \tanh(\phi)\dot{\phi}, \tag{10}$$

Taking the input saturation (5) into consideration, the positive design parameters k_1 and k_2 in (9) must be selected as

$$k_1 + k_2 \leq \tau_{\max}. \tag{11}$$

Then, in order to guarantee $\dot{V}$ in (10) is nonpositive, the auxiliary signal ϕ in (7) is designed as

$$\phi = v + k_2\theta, \tag{12}$$
$$\dot{v} = -k_2(v + k_2\theta), \tag{13}$$

where v is the output of the dynamic system (13). Substituting (12) and (13) into (10), it is straightforward to yield

$$\begin{aligned} \dot{V} &= -k_2 \tanh(\phi)\dot{\theta} + \tanh(\phi)(v + k_2\dot{\theta}) \\ &= \tanh(\phi)\dot{v} = -k_2\phi\tanh(\phi) \end{aligned} \tag{14}$$

According to the property of hyperbolic tangent function, it is known that $\dot{V}$ in (14) satisfies

$$\dot{V} \leq 0, \tag{15}$$

which indicates that

$$V(t) \leq V(0) \in \mathcal{L}_\infty, \quad \forall\, t \geq 0. \tag{16}$$

Therefore, the closed-loop control system under the proposed controller (9) is stable in the sense of Lyapunov, and all the state variables are bounded. However, there is no guarantee that the state variables converge to zeros, since $\dot{V}$ is negative semidefinite.

In order to further prove the asymptotic convergence of the state variables, define

$$\Omega = \left\{ (x, \dot{x}, \theta, \dot{\theta}) \mid V(t) \leq V(0) \right\}. \tag{17}$$

Substituting (9) into (1) and (2), the closed-loop system is simplified as

$$\dot{X} = F(X), \tag{18}$$

where $X = [x, \dot{x}, \theta, \dot{\theta}]^{\mathrm{T}}$. Then, any solution of (18) starting in Ω remains in Ω for all $t \geq 0$. Let Ψ be the invariant set in Ω:

$$\Psi = \left\{ (x, \dot{x}, \theta, \dot{\theta}) \mid \dot{V}(t) = 0 \right\}. \tag{19}$$

When $\dot{V}(t) = 0$, it follows from (14) and (19) that

$$\phi = 0 \Rightarrow \dot{\phi} = 0,\; \ddot{\phi} = 0. \tag{20}$$

Takingthe time derivative of (12) with (13) yields

$$\dot{\phi} = -k_2\phi + k_2\dot{\theta}. \tag{21}$$

Thus, it follows from (20) and (21) that

$$\dot{\theta} = 0,\; \ddot{\theta} = 0 \Rightarrow \theta = c, \tag{22}$$

where c is a constant, which is to be determined later. Substituting (22) into (9) yields

$$\tau = -k_1 \sin(0.5c), \tag{23}$$

Combining the dynamics (1) and (2) with (22) and (23) yields

$$\ddot{x} = -\frac{k}{M+m}x, \tag{24}$$
$$mr\ddot{x}\cos c = -k_1 \sin(0.5c). \tag{25}$$

Substituting (24) into (25) and making some arrangements yields

$$kxmr\cos c = k_1(M+m)\sin(0.5c). \tag{26}$$

Assume that $\cos c = 0$, i.e., $c = \frac{2n+1}{2}\pi$, then (26) becomes

$$k_1 \sin(0.5c) = 0. \tag{27}$$

Since $k_1 > 0$, it follows from (27) that $c = 2n\pi$, which contradicts the assumption of $\cos c = 0$. Hence, $\cos c \neq 0$.

Dividing both sides of (26) with $mr\cos c$ yields

$$kx = \frac{k_1(M+m)\sin(0.5c)}{mr\cos c}. \tag{28}$$

Notice that the right side of (28) is a constant, thus x is also a constant, which means that

$$\dot{x} = 0, \quad \ddot{x} = 0. \tag{29}$$

Substituting (29) into (24) yields

$$x = 0. \tag{30}$$

Furthermore, combining (28) with (30) yields

$$\sin(0.5c) = 0 \Rightarrow \theta = 2n\pi. \tag{31}$$

Therefore, the largest invariant set of (18) is expressed as

$$\mathcal{M} = \left\{ (x, \dot{x}, \theta, \dot{\theta}) \mid x = 0, \ \dot{x} = 0, \ \theta = 2n\pi, \ \dot{\theta} = 0 \right\}. \tag{32}$$

According to LaSalle's invariance theorem [45], every solution of (18) starting in Ω approaches to $\mathcal{M}$ with $t \to \infty$, that is, the control objective is realized.

In addition, since $|\tanh(*)| \leq 1$, from (9) and (11), it is clear that $|\tau| \leq \tau_{\max}$, i.e., the physical control input constraint (5) is satisfied. Furthermore, no velocity feedback information is needed in (9), which indicates that the designed controller only involves output feedback.

Summarizing the above results leads to the following stability theorem.

Theorem 1. *Consider the underactuated horizontal TORA systems (1) and (2). Let $\mathcal{M}$ be the largest invariant set of (18). Ω is a compact closed and bounded set that contains all the initial states of (18), and Ψ is a set of states in Ω where $\dot{V}(t) = 0$. If the control law (9) is employed, then all the state variables of the TORA system are bounded and converge to the largest invariant set $\mathcal{M}$ defined in (32) as $t \to \infty$, i.e.,*

$$\lim_{t\to\infty} [x, \ \dot{x}, \ \theta, \ \dot{\theta}]^{\mathrm{T}} = [0, \ 0, \ 2n\pi, \ 0]^{\mathrm{T}}. \tag{33}$$

In addition, the proposed controller only requires the output θ for feedback, and the control input is constrained as (5).

Remark 1. *There are only two control gains k_1, k_2 needed to tune in the proposed controller, which makes the control algorithm very easy to implement in engineering. To meet the input constraint, these two parameters must be selected satisfying (11) and tuned properly by trial and error. Generally speaking, a large k_1 value results in a short convergence time, but undesired oscillations appear in x and θ. In contrast, a large k_2 value produces a long convergence time, and less oscillations arise in x and θ. In accordance with the these rules, these two control values can be finally determined.*

4. Simulation Results

This section uses Matlab/Simulink to perform simulation tests to verify the effectiveness and superiority of the proposed control method.

The physical parameters of the horizontal TORA system are as follows:

$$M = 5.4 \text{ kg}, \ m = 0.96 \text{ kg}, k = 190 \text{ N/m}, r = 0.6 \text{ m}, J = 0.0022 \text{ kg} \cdot \text{m}^2. \tag{34}$$

Thecontrol gains in (9) is selected by trial and error as

$$k_1 = 2.7, \ k_2 = 3.3. \tag{35}$$

The maximum control input that the actuator can provide is

$$\tau_{\max} = 6 \text{ N} \cdot \text{m}. \tag{36}$$

Obviously, the selected control gains (35) satisfy the saturation constraint (5). The initial state of the system is set as

$$[x(0), \ \dot{x}(0), \ \theta(0), \ \dot{\theta}(0)]^{\text{T}} = [0.5, \ 0, \ 0, \ 0]^{\text{T}}. \tag{37}$$

4.1. Comparison Study

In order to highlight the superiority of the designed controller, the simulation results of the proposed controller are compared with those of controllers in [28,34].

The cascade-based controller proposed in [28] is

$$\begin{cases} u = \dfrac{-\alpha_2 z_3 + \alpha_1 \varepsilon W(z_1, z_2, z_3) z_1 \cos z_3 - \gamma z_4}{\alpha_3} \\ \tau = \dfrac{(M+m)(mr^2 + J) - m^2 r^2 \cos^2 \theta}{M+m} u + \dfrac{(mr\dot{\theta}^2 \sin \theta - kx)mr \cos \theta}{M+m} \end{cases} \tag{38}$$

where $\alpha_i (i = 1, 2, 3)$, γ, ε are positive control parameters, $z_i (i = 1, \cdots, 4)$ are new state variables transformed from $(x, \dot{x}, \theta, \dot{\theta})$, and $W(z_1, z_2, z_3)$ is a nonlinear function. For brevity, the detailed expressions of transformation coordinates and $W(z_1, z_2, z_3)$ are omitted here, interested readers are referred to [28] for details. The control parameters are chosen as the same as [28], i.e., $\alpha_1 = 5000, \alpha_2 = 100, \alpha_3 = 1, \gamma = 5, \varepsilon = 5.9306$.

The passivity-based controller proposed in [34] is

$$\begin{cases} \tau = -k_1 \tanh \theta - k_2 \tanh(\psi + b\theta) \\ \dot{\psi} = -ak_2 \tanh(\psi + b\theta) \end{cases} \tag{39}$$

where k_1, k_2, a, b are positive control parameters, ψ is an auxiliary function. After carrying out a lot of simulations, they are determined as $k_1 = 4, k_2 = 2, a = 10, b = 10$.

The simulation results of the TORA under the three control methods are depicted in Figures 2–4, which record the curves of cart position, ball angle and control torque, respectively. More details of quantified comparison indexes of the three control methods are presented in Table 1, where t_s, θ_p and τ_{cmax} represents the settling time, the maximum overshoot of the ball angle and the maximum control torque required by the controller, respectively.
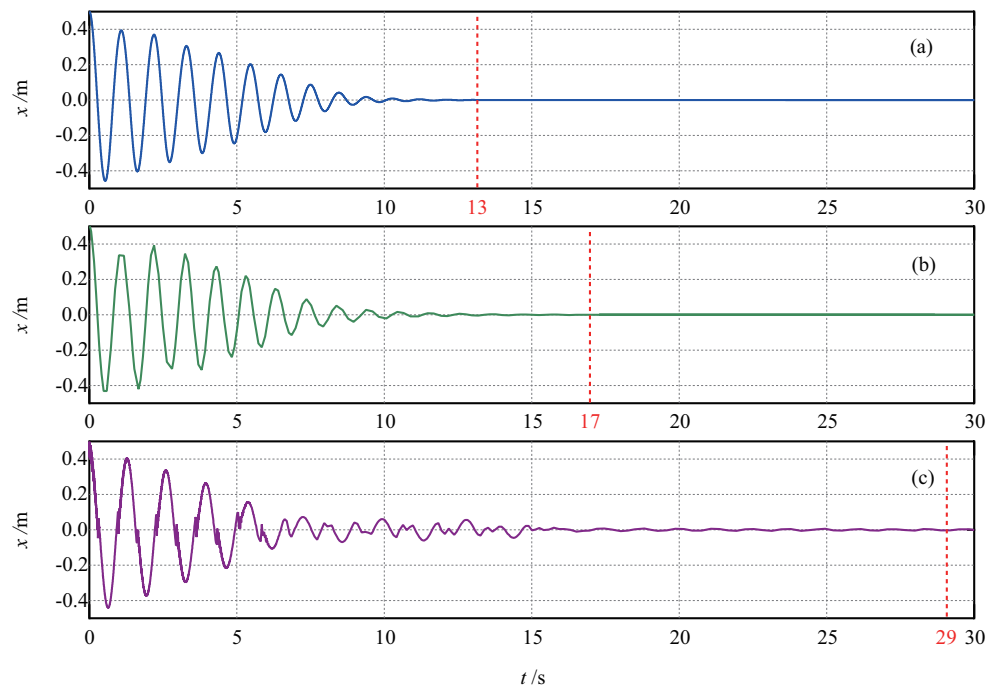
Figure 2. Time response curves of the cart position x. (**a**) Proposed method; (**b**) Method in [34]; (**c**) Method in [28].

Table 1. Quantified indexes of comparison results.

Control Methods	t_s (s)	θ_p (rad)	τ_{cmax} (N $\cdot$ m)
Proposed controler (9)	13	1.55	5.05
Controller (39) in [34]	17	1.74	5.75
Controller (38) in [28]	29	9.27	1.04×10^5
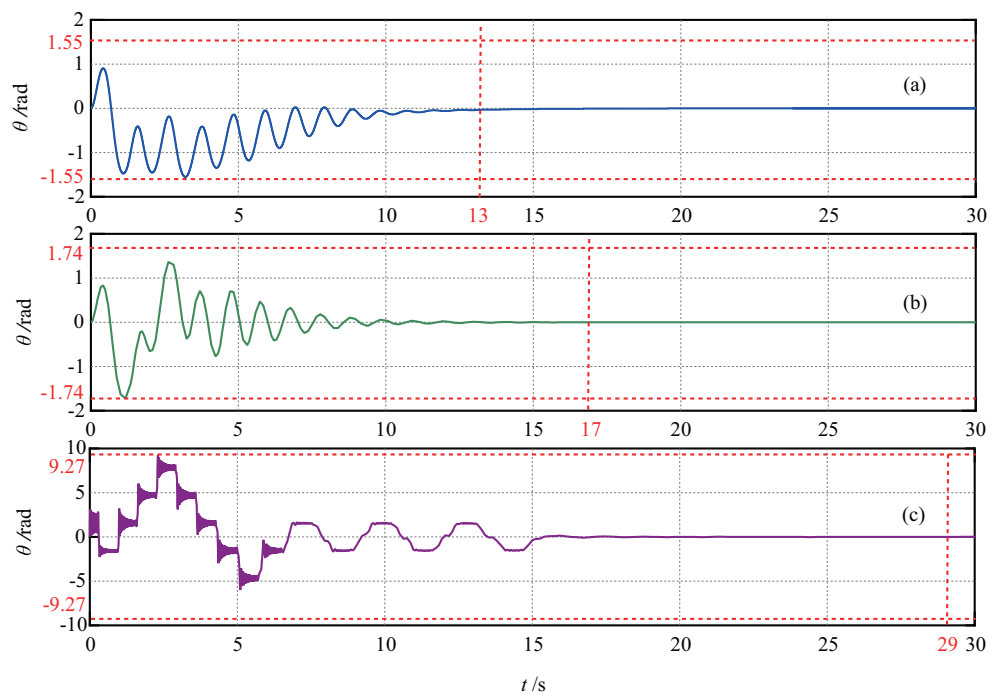
Figure 3. Time response curves of the ball rotational angle θ. (**a**) Proposed method; (**b**) Method in [34]; (**c**) Method in [28].
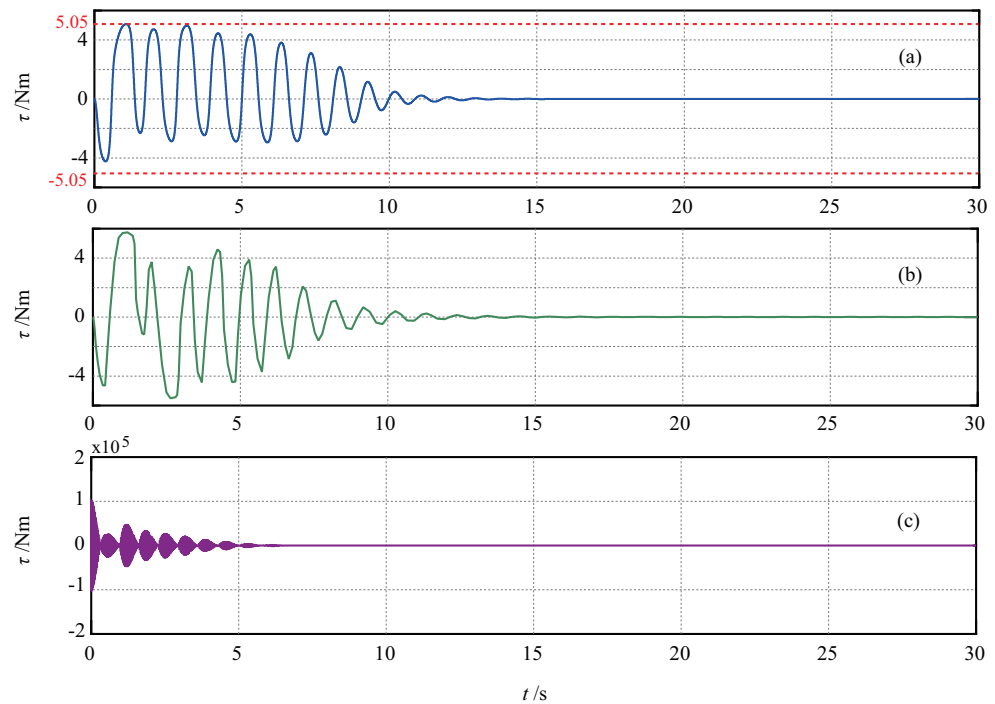
Figure 4. Time response curves of the control torque τ. (**a**) Proposed method; (**b**) Method in [34]; (**c**) Method in [28].

From these simulation results, it is observed that the translational position and rotational angle of the TORA system under the three control methods can be stabilized at the equilibrium point. However, from the quantified comparison index results in Table 1, we find that the control performance of the proposed control method is superior to the other two methods. Firstly, the settling time t_s of the proposed method is shortest among the three methods, which means the system is stabilized at the origin faster than the other two methods. Secondly, the maximum overshoot of the ball angle θ is smaller than that of the comparative methods. Lastly and most importantly, the control torque of the proposed control method is always within the constrained range, i.e., $|\tau| \leq 6\,\text{N} \cdot \text{m}$. In contrast, the required control torque in [28] is up to $1.04 \times 10^5\,\text{N} \cdot \text{m}$, which is not reasonable in practise. In addition, the proposed control method achieves a smoother transient control performance.

4.2. Robustness Test

In order to test the robustness of the proposed method, two different external disturbances and several parameter perturbations are imposed on the system. The first disturbance is a time-varying sinusoid disturbance, $d(t) = \sin(4\pi t)$, which is added from 25 s to 26 s. The other one is a white noise with a mean value of 0 and a variance of 1, which is added from 35 s to 40 s. The parameter perturbations are: $\triangle M = +10\%M$, $\triangle m = +10\%m$, $\triangle J = -10\%J$, $\triangle k = -10\%k$. The initial state is also chosen as $[x(0)\ \dot{x}(0)\ \theta(0)\ \dot{\theta}(0)]^{\mathrm{T}} = [0.5\ 0\ 0\ 0]^{\mathrm{T}}$.

The simulation results are given in Figure 5. From Figure 5, it is observed that the translational cart position and the rotational ball angle are stabilized at the origin almost at the same time as the nominal circumstance, even though there exist parameter uncertainties. After 25 s, the TORA system is driven to deviate away from the equilibrium position slightly by the disturbances, but the proposed controller can attenuate them quickly and bring the cart and ball back to the equilibrium point. In addition, the required control torque is always restricted in the constrained range. This simulation demonstrates that the proposed control method has good robustness to external disturbances and parameter uncertainties.
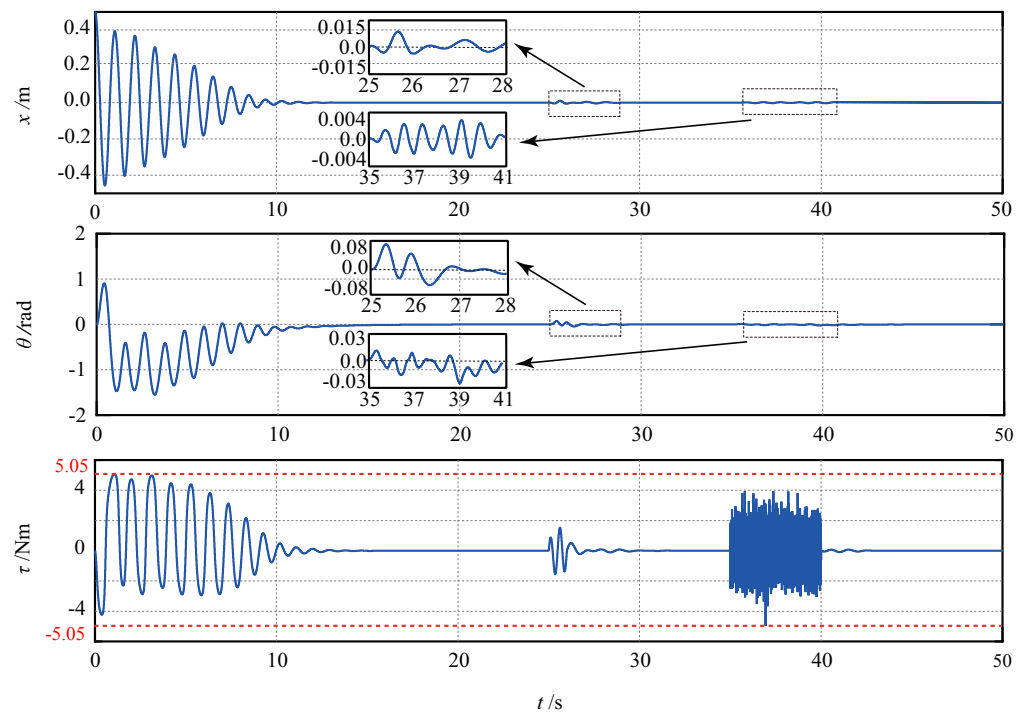
Figure 5. Simulation results of the TORA system with external disturbances and parameter uncertainties.

5. Conclusions

This paper proposed a novel amplitude-limited output feedback control approach to stabilize both the cart position and the eccentric ball angle of the underactuated TORA system at the equilibrium point. The proposed controller has a simple structure with no system parameters involved, which not only makes the control algorithm easy to implement in engineering, but also improves the robustness to parameter uncertainties. More importantly, the stabilization objective is realized with no velocity feedback and the required control torque never exceeds the amplitude-limited constraint that the actuator can provide. Rigorous theoretical analysis is presented to guarantee the asymptotic stability of the entire control system. The simulation and comparison results show that the proposed control approach archives a better control performance, including settling time, transient performance and robust to external disturbances.

It is worth mentioning that although the practical issues of velocity unavailability, input saturation and accurate model-knowledge requirements are tackled in the proposed control approach, some other practical factors such as full-state constraints [20,21], plant uncertainties and actuator dead zones [22] are not considered. In order to extend the application of the proposed control method, we will devote to investigating these practical factors in our future work. Moreover, we plan to build a physical TORA experimental platform to verify the control performance of the proposed approach.

Author Contributions: Conceptualization, C.P. and C.C.; methodology, C.C.; software, C.C.; validation, C.P., C.C. and P.X.; formal analysis, Z.L.; investigation, C.P.; resources, C.P.; data curation, P.X.; writing—original draft preparation, C.C.; writing—review and editing, C.P. and L.Z.; visualization, Z.L.; supervision, C.P.; project administration, C.P.; funding acquisition, C.P. All authors have read and agreed to the published version of the manuscript.

Institutional Review Board Statement: Not applicable.

Informed Consent Statement: Not applicable.

Data Availability Statement: Not applicable.

Conflicts of Interest: The authors declare no conflict of interest.

References

1. Bupp, R.T.; Bernstein, D.S.; Coppola, V.T. A benchmark problem for nonlinear control design. *Int. J. Robust Nonlinear Control* **1998**, *8*, 307–310. [CrossRef]
2. Fradkov, A.; Tomchina, O.; Tomchin, D. Controlled passage through resonance in mechanical systems. *J. Sound Vib.* **2011** *330*, 1065–1073. [CrossRef]
3. Sun, N.; Wu, Y.; Fang, Y.; Chen, H. Nonlinear Stabilization Control of Multiple-RTAC Systems Subject to Amplitude-Restricted Actuating Torques Using Only Angular Position Feedback. *IEEE Trans. Ind. Electron.* **2017**, *64*, 3084–3094. [CrossRef]
4. Shah, S.A.A.; Gao, B.; Ahmed, N.; Liu, C. Advanced robust control techniques for the stabilization of translational oscillator with rotational actuator based barge-type OFWT. *Proc. Inst. Mech. Eng. Part M J. Eng. Marit. Environ.* **2021**, *235*, 327–343. [CrossRef]
5. Zhang, Y.; Li, L.; Cheng, B.; Zhang, X. An active mass damper using rotating actuator for structural vibration control. *Adv. Mech. Eng.* **2016**, *8*, 1–9. [CrossRef]
6. He, M.E.; Hu, Y.Q.; Zhang, Y. Optimization design of tuned mass damper for vibration suppression of a barge-type offshore floating wind turbine. *Proc. Inst. Mech. Eng. Part M J. Eng. Marit. Environ.* **2017**, *231*, 302–315. [CrossRef]
7. Wu, Y.; Sun, N.; Fang, Y.; Liang, D. An increased nonlinear coupling motion controller for underactuated Multi-TORA systems: Theoretical design and hardware experimentation. *IEEE Trans. Syst. Man Cybern. Syst.* **2019**, *49*, 1186–1193. [CrossRef]
8. Liu, Y.; Yu, H.N. A survey of underactuated mechanical systems. *IET Control Theory Appl.* **2013**, *7*, 921–935. [CrossRef]
9. He, B.; Wang, S.; Liu, Y.J. Underactuated robotics: A review. *Int. J. Adv. Robot. Syst.* **2019**, *16*, 1729881419862164. [CrossRef]
10. Chen, T.; Goodwine, B. Controllability and accessibility results for N-link horizontal planar manipulators with one unactuated joint. *Automatica* **2021**, *125*, 109480. [CrossRef]
11. Wang, L.; Chen, S.; Zhang, P.; She, J.; Lai, X. A Simple Control Strategy Based on Trajectory Planning for Vertical Acrobot. *Actuators* **2021**, *10*, 308. [CrossRef]
12. Chen, S.; Wang, Y.; Zhang, P.; Su, C.Y. Continuous Control Strategy of Planar 3-Linkage Underactuated Manipulator Based on Broad Neural Network. *Actuators* **2021**, *10*, 249. [CrossRef]
13. Yao, X.Y.; Park, J.H.; Ding, H.F.; Ge, M.F. Event-triggered consensus control for networked underactuated robotic systems. *IEEE Trans. Cybern.* **2020**, *early access*. [CrossRef] [PubMed]
14. Wang, L.; Lai, X.; Meng, Q.; Wu, M. Effective Control Method Based on Trajectory Optimization for Three-Link Vertical Underactuated Manipulators With Only One Active Joint. *IEEE Trans. Cybern.* **2021**, *early access*. [CrossRef]
15. Quan, Q.; Cai, K.Y. Additive-state-decomposition-based tracking control for benchmark. *J. Sound Vib.* **2013**, *332*, 4829–4841. [CrossRef]
16. Wu, X.; Zhao, Y.; Xu, K. Nonlinear disturbance observer based sliding mode control for a benchmark system with uncertain disturbances. *ISA Trans.* **2021**, *110*, 63–70. [CrossRef] [PubMed]
17. Sun, N.; Wu, Y.; Fang, Y.; Chen, H.; Lu, B. Nonlinear Continuous Global Stabilization Control for Underactuated RTAC Systems: Design, Analysis, and Experimentation. *IEEE/ASME Trans. Mechatron.* **2017**, *22*, 1104–1115. [CrossRef]
18. Wu, X.; Xu, K.; Ma, M.; Ke, L. Output feedback control for an underactuated benchmark system with bounded torques. *Asian J. Control* **2021**, *23*, 1466–1475. [CrossRef]
19. Jiang, Z.P.; Kanellakopoulos, I. Global output feedback tracking for a benchmark nonlinear system. *IEEE Trans. Autom. Control* **2000**, *45*, 1023–1027. [CrossRef]
20. Yang, T.; Sun, N.; Fang, Y. Neuroadaptive control for complicated underactuated systems with simultaneous output and velocity constraints exerted on both actuated and unactuated states. *IEEE Trans. Neural Netw. Learn. Syst.* **2021**, *early access*. [CrossRef]
21. Yang, T.; Chen, H.; Sun, N.; Fang, Y. Adaptive neural network output feedback control of uncertain underactuated systems with actuated and unactuated state constraints. *IEEE Trans. Syst. Man Cybern. Syst.* **2021**, *early access*. [CrossRef]
22. Yang, T.; Chen, H.; Sun, N.; Fang, Y. Adaptive fuzzy control for a class of MIMO underactuated systems with plant uncertainties and actuator deadzones: Design and experiments. *IEEE Trans. Cybern.* **2021**, *early access*. [CrossRef] [PubMed]
23. Lee, C.H.; Chang, S.K. Experimental implementation of nonlinear TORA system and adaptive backstepping controller design. *Neural Comput. Appl.* **2012**, *21*, 785–800. [CrossRef]
24. Liu, D.; Guo, W. Nonlinear backstepping design for the underactuated TORA system. *J. Vibroengineering* **2014**, *16*, 552–559.
25. Guo, W.; Liu, D. Nonlinear dynamic surface control for the underactuated translational oscillator with rotating actuator system. *IEEE Access* **2019**, *7*, 11844–11853. [CrossRef]
26. Wu, T.; Gui, W.; Hu, D.; Du, C. Adaptive fuzzy sliding mode control for translational oscillator with rotating actuator: A fuzzy model. *IEEE Access* **2018**, *6*, 55861–55869. [CrossRef]
27. Wu, X.; Xu, K. Global sliding mode control for the underactuated translational oscillator with rotational actuator system. *Proc. Inst. Mech. Eng. Part I J. Syst. Control Eng.* **2021**, *235*, 540–549. [CrossRef]
28. Zhang, A.C.; She, J.H.; Qiu, J.D. A new control method for global stabilisation of translational oscillator with rotational actuator. *Int. J. Syst. Sci.* **2019**, *50*, 954–960. [CrossRef]

29. Gao, B.T. Dynamic modeling and energy-based control design for TORA. *Acta Autom. Sin.* **2008**, *34*, 1221–1224. [CrossRef]
30. Wu, X.Q.; Gu, M.M. Adaptive control of the TORA system with partial state constraint. *Trans. Inst. Meas. Control* **2019**, *41*, 1172–1177. [CrossRef]
31. Burg, T.; Dawson, D. Additional notes on the TORA example: A filtering approach to eliminate velocity measurements. *IEEE Trans. Control Syst. Technl.* **1997**, *5*, 520–523. [CrossRef]
32. Escobar, G.; Ortega, R.; Sira-Ramrez, H. Output-feedback global stabilization of a nonlinear benchmark system using a saturated passivity-based controller. *IEEE Trans. Control Syst. Technol.* **1999**, *7*, 289–293. [CrossRef]
33. Gao, B.; Xu, J.; Zhao, J.; Huang, X. Stabilizing control of an underactuated 2-dimensional TORA with only rotor angle measurement. *Asian J. Control* **2013**, *15*, 1477–1488. [CrossRef]
34. Gao, B.; Bao, Y.; Xie, J.; Jia, L. Passivity-based control of two-dimensional translational oscillator with rotational actuator. *Trans. Inst. Meas. Control* **2014**, *36*, 111–118. [CrossRef]
35. Gao, B.; Ye, F. Fuzzy Lyapunov synthesis control of an underactuated 2DTORA system. *J. Intell. Fuzzy Syst.* **2015**, *28*, 581–589. [CrossRef]
36. Xu, K.; Wu, X.; Ma, M.; Zhang, Y. Energy-based output feedback control of the underactuated 2DTORA system with saturated inputs. *Trans. Inst. Meas. Control* **2020**, *42*, 2822–2829. [CrossRef]
37. Zheng, G.B.; Gao, B.T.; Liu, C.D. Fuzzy control design of periodic dynamic trajectory of TORA system. *Control Eng.* **2019**, *26*, 1029–1034.
38. Liu, C.; Gao, B.; Zheng, G.; Sun, G. Fuzzy control design of oscillating trajectory tracking for underactuated TORA. *Electr. Mach. Control* **2018**, *22*, 117–122.
39. Avis, J.M.; Nersesov, S.G.; Nathan, R. A comparison study of nonlinear control techniques for the RTAC system. *Nonlinear Anal. Real World Appl.* **2010**, *11*, 2647–2658. [CrossRef]
40. She, J.; Zhang, A.; Lai, X.; Wu, M. Global stabilization of 2-DOF underactuated mechanical systems-an equivalent-input-disturbance approach. *Nonlinear Dyn.* **2012**, *69*, 495–509. [CrossRef]
41. He, S.; Ji, H.; Yang, K. Semi-global output feedback tracking to reference system with input for a benchmark nonlinear system. *Asian J. Control* **2019**, *21*, 749–758. [CrossRef]
42. Qi, Z.; Li, H.; Wu, C. Adaptive Fuzzy Control of Nonlinear Systems With Unmodeled Dynamics and Input Saturation Using Small-Gain Approach. *IEEE Trans. Syst. Man Cybern. Syst.* **2017**, *47*, 1979–1989.
43. Zheng, Z.; Sun, L. Path following control for marine surface vessel with uncertainties and input saturation. *Neurocomputing* **2016**, *177*, 158–167. [CrossRef]
44. Bupp, R.T.; Bernstein, D.S.; Coppola, V.T. Experimental implementation of integrator backstepping and passive nonlinear controllers on the RTAC tested. *Int. J. Robust Nonlinear Control* **1998**, *8*, 435–457. [CrossRef]
45. Khalil, H.K. *Nonlinear Systems,* 3rd ed.; Prentice Hall: Upper Saddle River, NJ, USA, 2002.